[redacted]

N64 13280
CODE-1
CR-53017

Technical Report No. 32-512

# Criticality Calculations for a Fast Liquid-Metal-Cooled Reactor—Phase I

H. G. Gronroos

OTS PRICE

XEROX $ 2.60 ph.

MICROFILM $ 1.01 mf.

JET PROPULSION LABORATORY
CALIFORNIA INSTITUTE OF TECHNOLOGY
PASADENA, CALIFORNIA

November 15, 1963

~~Technical Report No. 32-512~~

# Criticality Calculations for a Fast Liquid-Metal-Cooled Reactor—Phase I

H. G. Gronroos 15 Nov. 1963 27p refs

☒ OTS

2

(NASA Contract NAS7-100)

(NASA CR-53017; JPL-TR-32-512) OTS: $2.60ph $1.00mf

John J. Paulson
J. J. Paulson, Chief
Advanced Propulsion Engineering Section

4742003

JET PROPULSION LAB[redacted]Y
CALIF[redacted]A INST[redacted] OF TECH[redacted]Y
PASADENA, [redacted]A

~~November 15, 1963~~

Copyright © 1963
Jet Propulsion Laboratory
California Institute of Technology

Prepared Under Contract No. NAS 7-100
National Aeronautics & Space Administration

## CONTENTS

**I. Introduction** . . . . . 1

**II. The Conceptual Design** . . . . . 3

A. Materials Specification . . . . . 6

B. Dimensions and Volumes as Functions of Temperature . . . . . 7

**III. Criticality Calculations** . . . . . 10

A. The *AIM*-6 Code . . . . . 11

B. Multigroup Cross-sections. . . . . 12

C. Some Basic Criticality Calculations. . . . . 12

**IV. Results of Parameter Studies**. . . . . 14

A. Choice of Natural Li or $Li^7$ as Primary Coolant and Slurry Liquid . . . . . 14

B. Radial and Axial Power Shape Factors and Power Generation Distributions . . . . . 14

C. Reflector Worth . . . . . 15

D. Neutron Spectrum Distributions . . . . . 16

E. Influence of Constructional Components. . . . . 16

F. Temperature Coefficients . . . . . 17

**V. Conclusion**. . . . . 19

**References** . . . . . 20

## TABLES

1. **Reactor characteristics** . . . . . 3

2. **Core, primary, and secondary loop characteristics**. . . . . 4

3. **Dimensions at 68°F, material composition, and parameters subject to investigation** . . . . . 5

4. **Reactor component temperatures at points of particular interest** . . . . 7

5. **Materials constants used in calculating volumes, dimensions, and atomic densities** . . . . . 7

6. **Neutron flux in reactor core. Normalized to 1w thermal power** . . . . 17

7. **Reactor physics properties of reactor in Fig. 2** . . . . . 19

# FIGURES


1. 10 Mwth reactor assembly . . . . . 2
2. 10 Mwth fast reactor . . . . . 3
3. Temperature of reactor components as a function of fuel temperature . . . . . 6
4. Linear thermal expansion coefficient for Uranium Carbide (Ref. 6) . . . 8
5. Linear thermal expansion coefficient $\alpha_i$ (20°C → T°C) for Uranium Carbide, Beryllium and Niobium . . . . . 8
6. Lithium and Potassium density as a function of temperature (Ref. 7) . . 8
7. Density as a function of temperature for Nb-1% Zr, UC and BeO . . . 8
8. Average Li density in core as a function of fuel temperature and slurry concentration . . . . . 9
9. Increase in core dimensions and volume as a function of core vessel temperature . . . . . 9
10. Volume fractions of UC, Li and Nb-1% Zr as functions of fuel temperature and slurry concentration . . . . . 9
11. The effective multiplication as a function of the transverse leakage and fuel slurry concentration . . . . . 13
12. Mass $U^{235}$ and required burnup as a function of fuel slurry concentration . . . . . 13
13. Peak power/average power ratios as functions of transverse buckling and fuel slurry concentration . . . . . 14
14. Power generation ratios vs core radius and core height . . . . . 15
15. Reflector worth as a function of the axial buckling and fuel slurry concentration . . . . . 15
16. Proposed reflector construction to improve power shape factors and control characteristics . . . . . 16
17. Reactivity changes vs thickness of axial structural components . . . . 18
18. Total and differential delayed temperature coefficients . . . . . 18

# PREFACE

The work reported herein represents part of the reactor physics investigations of a nuclear reactor concept for electric propulsion application. At present, the main objective is to calculate the following:

1. Critical mass and size
2. Power distribution in space and time
3. Reactivity changes
4. Reflector worth
5. Energy distribution of flux
6. Prompt and delayed temperature coefficients

The emphasis is at present placed on general survey calculations and aimed at determining the characteristics of the reactor. However, the accuracy should be such that gross changes in the design concept will not occur because of more sophisticated analysis.

The long range objectives consist of establishing the techniques of analysis necessary for carrying the physics calculations to as high a degree of accuracy as is presently attainable. It is further desired to establish, in the form of appropriate cross-section sets and computer programs, a generalized, accurate, and readily usable technique for further studies.

## ABSTRACT

13280

Multigroup diffusion theory calculations have been employed to evaluate some static reactor physical properties for a conceptual fast liquid-metal-cooled reactor. Also, the influence of the constructional components on reactivity is investigated. It is concluded that the reactor concept holds promise in fulfilling the requirements of 20,000 hr of operation at 10 Mw thermal power with reflector control, provided 45,000 Mwday/ton burnup can be achieved with a uranium refractory and lithium fuel slurry at 2700°F peak fuel temperature.

AUTHOR

## I. INTRODUCTION

Earlier criticality and parameter calculations (Ref. 1), together with other pertinent investigations, led to the adoption of a conceptual fast reactor design for electric propulsion application. References 2 and 3 describe design, desired performance, task, and motivations for the particular choices.

This Report includes results from multigroup diffusion theory criticality and parameter calculations aimed at further clarifying the characteristics of the reactor. In particular, the influence of some constructional components on the overall performance has been investigated. The temperature dependence is analyzed only in a crude fashion. Future reports will deal with this aspect, as well as burnup and the kinetics of the reactor system.

The reactor physics calculations have not been carried to a high order, and substantial probable errors in the absolute $k_{eff}$ values are tolerated. However, the probable errors in the relative relationships are found to be acceptable for the present purposes. As is pointed out, final absolute adjustment can be achieved most simply by adjusting the fuel slurry concentration.

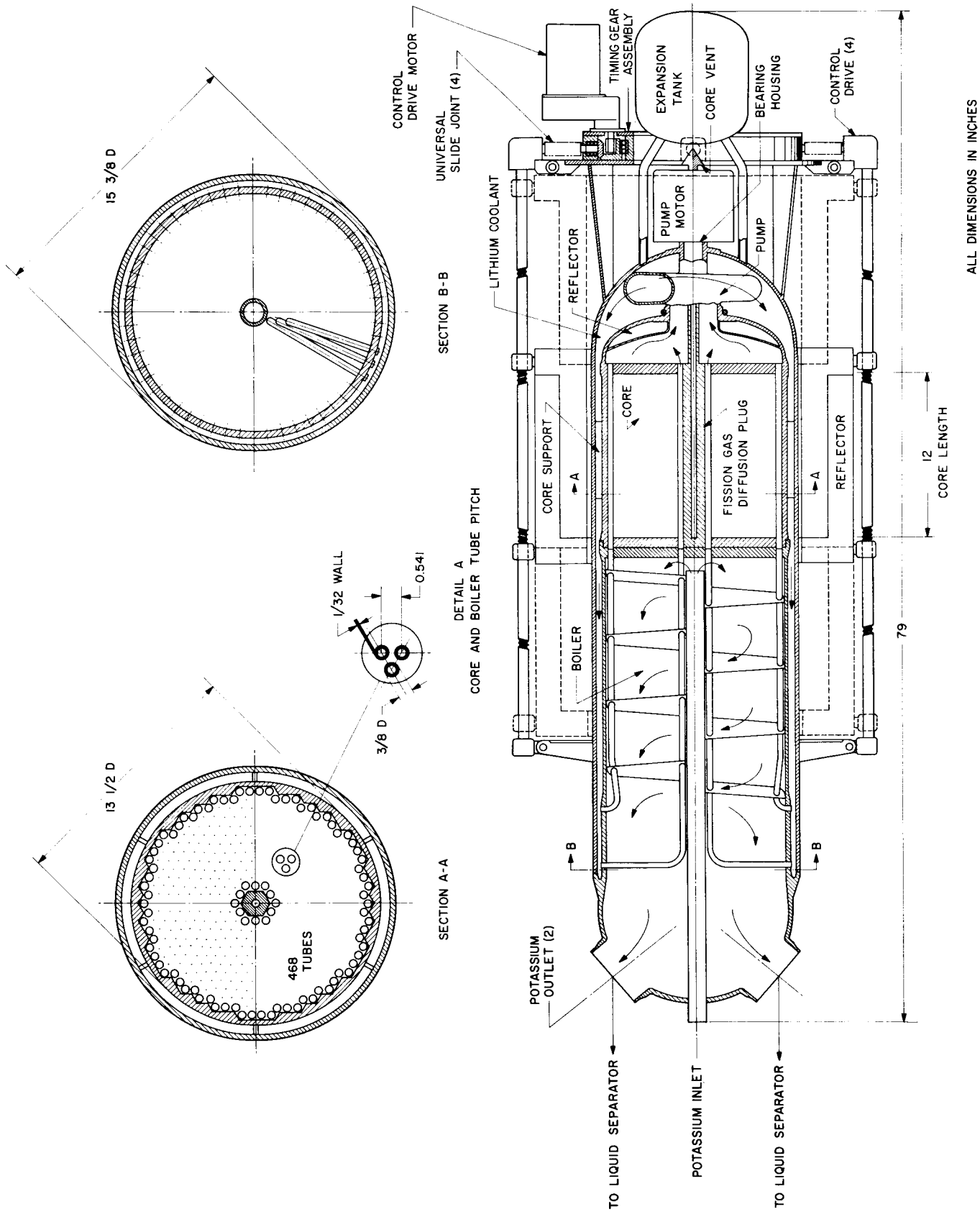


**Fig. 1. 10 *Mwth* reactor assembly**

# II. THE CONCEPTUAL DESIGN

Figure 1 shows the conceptual design and Tables 1 and 2 give some data for the system. In the calculations, the geometry is further simplified as indicated in Fig. 2. The core, core vessel endplates, radial coolant channel, and boiler are taken as homogenous mixtures of the material components. It is further assumed that the reflector and annular gap have uniform thickness over the core height. Because of this simplification, calculations are done only for the bare or fully reflected core. A complete analysis of a design with axially moving reflectors, from which some both constructionally and physically desirable features can be expected (Ref. 4), would call for sophistication beyond calculational methods employed here.

Table 3 displays systematically the various components and their dimensions at room temperature (68°F), to-

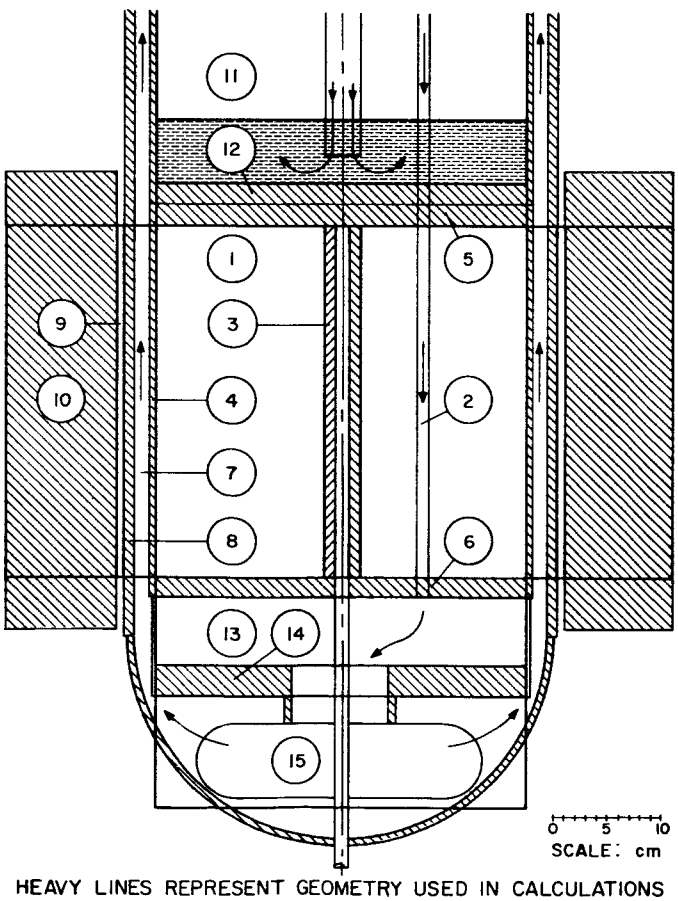


HEAVY LINES REPRESENT GEOMETRY USED IN CALCULATIONS
ITEMS DEFINED IN TABLE 3

**Fig. 2. 10 Mwth fast reactor**

**Table 1. Reactor characteristics**

| Item | Characteristic |
|---|---|
| Reactor type | Fast<br>Nonboiling<br>Liquid metal cooled |
| Fuel | Fully-enriched (93.5%) uranium refractory |
| Nuclear life, full-power hr | 20,000 |
| System life (design conditions), yr | 3 |
| Startup | Ground command<br>Steady-state preprogramming or manual control |
| Operation | Inherently load responsive<br>Satisfactory operation from self-sustaining to 100% design thermal power |
| Transient operation | Satisfactory response to instantaneous load-demand changes of at least 25% in power range |
| Basic structural material | Nb — 1% Zr |
| Allowable design stresses, psi | |
| Steady-state mechanical | 1,000 |
| Steady-state thermal | 5,000 |
| Cyclic thermal | 4,000 |
| Cold shock and vibration | 15,000 |
| Temperature, °F | |
| Structural design | 2100 |
| Maximum steady-state coolant (core hot channel exit) | 2100 |
| Criticality and reactivity insertion incidents | |
| Launch abort | Reactor shall be prevented from attaining criticality as a result of any launch abort incident |
| Ground handling | Sufficient cold shutdown reactivity margin to prevent attaining criticality from reasonably credible incidents |
| Reactivity insertion rate and scram | Reactivity insertion rate and scram protection shall prevent core damage resulting from any equipment or operational failures during ground testing |
| Dimensions and arrangements | Consistent with handling and launch vehicle constraints |

## Table 2. Core, primary, and secondary loop characteristics

**Core characteristics**

| Item | Value | Item | Value |
|---|---|---|---|
| Reactor thermal power, Mw | 10 | Heat transfer area, $ft^2$ | 46 |
| Fuel (slurry) | | Average heat flux, Btu/hr-$ft^2$ | $0.742 \times 10^6$ |
| Composition, vol % | | Power distribution | |
| UC | 80 | $F_{radial}$ | 1.3 |
| Li | 20 | $F_{axial}$ | 1.5 |
| Enrichment, % | | $F_{overall}$ | $1.3 \times 1.5 = 2$ |
| $U^{235}$ | 93.5 | Temperature uncertainty factors | |
| $U^{238}$ | 6.5 | $F_{wall}$ | 1.2 |
| UC m.p., °F | 4500 | $F_{film}$ | 1.3 |
| Li b.p. at 100 psia, °F | 3050 | $F_{fuel}$ | 1.25 |
| Coolant | Li | Hot channel factor $F_{HC}$ | 1.5 |
| $\Delta T$, °F | 80 | Temperatures, °F | |
| Size | | $\Delta T_{film}$ | 140 |
| Effective length, in. | 12 | $\Delta T_{film\ max}$ | 180 |
| Effective diameter, in. | 15 | $\Delta T_{wall}$ | 100 |
| Tubes | | $\Delta T_{wall\ max}$ | 120 |
| OD, in. | 3/8 | $\Delta T_{fuel}$ | 460 |
| Wall thickness, in. | 1/32 | $\Delta T_{fuel\ max}$ | 575 |
| Number | 468 | $\Delta T_{total}$ | 700 |
| Pitch, in. | 0.541 | $\Delta T_{total\ max}$ | 875 |
| Material of construction | Cb-1% Zr | Coolant temperature (HC midpoint), °F | 2040 |
| Heat-generation rate, | | Maximum fuel temperature (midcore), °F | 2915 |
| Mw/$ft^3$ | ~10 | Nominal HC fuel temperature (midcore), °F | 2740 |

**Primary loop characteristics**

| Item | Value |
|---|---|
| Fluid | Li |
| MP, °F | 357 |
| Vapor pressure at 2100°F, psia | 3.6 |
| Flow rate, lb/hr | $4.31 \times 10^5$ |
| Velocity, ft/sec | |
| Tubes | 17.9 |
| Annulus | 12.4 |
| Temperature, °F | |
| Inlet | 1980 |
| Outlet | 2060 |
| $\Delta T$, °F | 80 |
| Pressure | |
| Nominal, psia | 100 |
| $\Delta P_{reactor}$, psi | 1 |
| $\Delta P_{boiler}$, psi | 3 |
| $\Delta P_{loop}$, psi | 5 |
| Contingency, psi | 6 |
| Total, psi | 15 |
| Pumping power, hp | 17.5 |

**Secondary loop characteristics**

| Item | Value |
|---|---|
| Fluid | K |
| MP, °F | 146 |
| Boiler | |
| Operating temperature, °F | 1900 |
| Operating pressure, psia | 115 |
| Flow Rate, lb/hr | 46,200 |
| Vapor lines (2) | |
| ID | 5 |
| Velocity, ft/sec | 235 |
| Liquid line (1) | |
| ID, in. | 2 |
| Velocity, ft/sec | 15 |
| Pump work, hp | |
| Condensate pump | 1.1 |
| Feed pump | 8.8 |
| Quality, % | |
| Interstage | 91 |
| Exit | 92 |
| Boiler heat transfer area, $ft^2$ | 92 |
| Average heat flux, Btu/hr-$ft^2$ | 340,000 |
| Representative heat transfer coefficients, Btu/hr-$ft^2$ °F | |
| $h_{Li}$ | 12,000 |
| $h_K$ (liquid) | 4,500 |
| $h_K$ (boiling) | 4,600-11,000 |
| $U_{preheater\ section}$ | 2,370 |
| $U_{boiling}$ | 2,820-4,430 |

**Table 3. Dimensions at 68°F, material composition, and parameters subject to investigation**

| Item* | | Material composition | Dimension at 68°F, cm | Parameter investigated—remarks |
|---|---|---|---|---|
| 1 | Core: Height | | 32.60 | |
| | OD | | 34.00 | |
| | ID | | 3.40 | |
| | Fuel: Composition | 80 vol % UC + 20 vol % Li slurry | | UC concentration<br>Natural Li or $Li^7$ as slurry liquid |
| | Enrichment | 93.5 at. % $U^{235}$ in U | | |
| 2 | Coolant and coolant piping: | 468 pipes through core and boiler | | Natural Li or $Li^7$ as coolant |
| | OD | | 0.9525 (3/8 in.) | |
| | ID | | 0.7938 (5/16 in.) | |
| | Pitch (triangular) | | 1.374 (0.54 in.) | |
| | Wall | Nb-1% Zr | 0.07938 (1/32 in.) | |
| 3 | Diffusion plug: | 80% density of Nb-1% Zr | | The material composition and construction of this item has not yet been determined |
| | Cavity diameter | | 1.20 | |
| | OD | | 3.40 | |
| | Length | | 32.60 | |
| | Core vessel: | | | |
| | OD | | 35.20 | |
| | ID | | 34.00 | |
| 4 | Wall | Nb-1% Zr | 0.60 | |
| 5 | End plate at coolant entrance | Nb-1% Zr, Li coolant | 1.90 | $\delta k_{eff}$ as a function of plate thickness |
| 6 | End plate at coolant exit | Nb-1% Zr, Li coolant | 1.90 | $\delta k_{eff}$ as a function of plate thickness |
| 7 | Radial regions: | | | |
| | Coolant annulus | Li | 1.30 | Core vessel wall, coolant, and reactor vessel wall taken as homogenous mixture of thickness 2.60 cm |
| | Reactor vessel: | | | |
| | OD | | 39.20 | |
| | ID | | 37.80 | |
| | Height | | 32.60 | |
| 8 | Wall | | 0.70 | |
| 9 | Annular gap | vacuum | 0.90 | |
| 10 | Reflector: | | | $\delta k_{eff}$ as a function of reflector thickness |
| | Thickness | | 0-10.0 | |
| | Height | | 32.60 | |
| 11 | Boiler: | | | Primary and secondary coolant and piping taken as homogenous mixture |
| | Height | | 65.00 | |
| | Radius | | 34.00 | |
| | Coolant | K | | $\delta k_{eff}$ as a function of boiler operation |
| 12 | Boiler end plate | Nb-1% Zr | 1.80 | Core vessel and boiler end plates and coolant taken as homogenous mixture of thickness 3.70 cm<br>$\delta k_{eff}$ as a function of thickness |
| 13 | Coolant exit: | | | |
| | Coolant space | Li | 6.40 | |
| 14 | Reflector | BeO | 3.00 | Reflector influence on $k_{eff}$ |
| 15 | Coolant pump space | Li | 10.00 | Pump material not taken into account |

*Item number from Fig. 2.

gether with parameters subject to this study. Parameter influences to be determined are:

1. Choice of natural Li or $Li^7$ as primary coolant and slurry liquid
2. Influence of fuel concentration on reactivity
3. Reflector worth
4. Influence of boiler construction and operation on reactivity
5. Influence of the axial construction at the coolant exit side on reactivity
6. Influence of the central cavity and diffusion wall on reactivity
7. Reactivity changes as a function of temperature

A desirable feature would be one in which changes in the boiler condition would not significantly influence the reactivity, thus giving more stability and safety to the reactor operation. It would also be simpler to completely omit the reflector at the coolant exit side. These improvements are discussed below.

It is assumed that the radial reflectors are at 1900°F temperature at full power operation. The temperatures of the different components are taken to be linearly dependent on the fuel temperature in proportion to the given full power values. Figure 3 illustrates the simplified distributions assumed for the system. All Li and K becomes liquid at a fuel temperature of 460°F. This value is arrived at assuming $\Delta T_{\text{film}} + \Delta T_{\text{wall}} = 190°\text{F}$ for all temperatures in the boiler.

At full power, the thickness of the liquid potassium layer at the reactor end is about 7 cm (Ref. 5), and the density of the potassium vapor varies according to the following equation (Ref. 4):

$$v = v_f(\ell - x), -v_g x,$$

where

$v_g = 5\ \text{ft}^3/\text{lb}$ at 1900°F

$v_f = 0.026\ \text{ft}^3/\text{lb}$ at 1900°F

$x = 0.85\ \ell/L$

$L = 58$ cm

= height of vapor region in the boiler

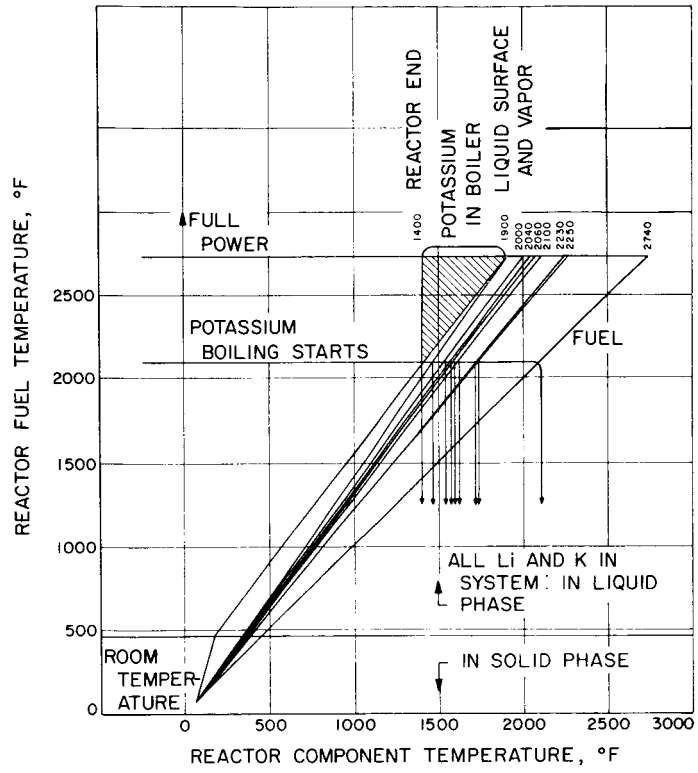


**Fig. 3. Temperature of reactor components as a function of fuel temperature**

and

$\ell$ = height coordinate in vapor region measured from the reactor core end

Each item is given a spatially constant temperature value, and higher order corrections to the neutron diffusion due to actually existing temperature distributions are ignored. In Table 4, values at some particularly interesting temperature points are given.

## A. Materials Specification

The constants used for calculating the volumes, dimensions, and atomic densities are given in Table 5 and Figs. 4, 5 and 6. The values represent what have been considered best choices from data reported in the literature.

For UC, it is assumed that 98% of the theoretical density can be achieved with arc-cast material containing 5 wt%C. The upper curve of the thermal expansion coefficient functions given in Fig. 5 should be used. This curve is actually for sintered UC, but since, in applica-

**Table 4. Reactor component temperatures at points of particular interest**

| | Item* | Li and K melting, °F | Potassium boiling, °F | Full power, °F |
|---|---|---|---|---|
| 1 | Fuel slurry | 460 | 2100 | 2740 |
| 2 | Coolant in core | 360 | 1570 | 2040 |
| 2 | Coolant pipe wall in core | 380 | 1720 | 2230 |
| 3 | Diffusion plug | 460 | 1900 | 2740 |
| 4 | Core vessel wall | 380 | 1740 | 2250 |
| 5 | End plate at coolant entrance | 360 | 1620 | 2100 |
| 6 | End plate at coolant exit | 380 | 1740 | 2250 |
| 7 | Coolant annulus | 360 | 1590 | 2060 |
| 8 | Reactor vessel wall | 350 | 1540 | 2000 |
| 10 | Reflector | 330 | 1470 | 1900 |
| 11 | Potassium in boiler | 170 | 1400 | 1400-1900 |
| 12 | Boiler end plate | 360 | 1620 | 2100 |
| 13 | Coolant space | 360 | 1590 | 2060 |
| 14 | Reflector | 360 | 1590 | 2060 |
| 15 | Coolant pump space | 360 | 1590 | 2060 |

*Item number from Fig. 2.

**Table 5. Materials constants used in calculating volumes, dimensions, and atomic densities**

| Item | Specification | Density at 68°F, g/cm³ | Thermal expansion | Atomic weight, amu | Remarks |
|---|---|---|---|---|---|
| Construction material | 99 wt % Nb<br>1 wt % Zr | Nb = 8.57<br>Zr = 6.51<br>Nb-1% Zr = 8.54 (calc) | Fig. 5 | Nb = 92.91<br>Zr = 91.22<br>Nb-1% = 92.89 (calc) | Thermal expansion coefficient for 100 wt % Nb used |
| Fuel | 5 at. % C<br>95 at. % U<br>93.5 at. % U in U | 13.23 (calc) | Fig. 4<br>Fig. 5 | $U^{235}$ = 235.12<br>$U^{238}$ = 238.13<br>$C^{12}$ = 12.01<br>UC = 247.40 | ±10% error in thermal expansion coefficient |
| Primary coolant and slurry solvent | Lithium<br>92.5 at. % $Li^7$<br>7.5 at. % $Li^6$ | 0.534 for elemental Li | Fig. 6 | $Li^6$ = 6.0170<br>$Li^7$ = 7.0182<br>Li = 6.0170 | |
| Reflectors | Beryllia<br>BeO | 2.80 | Fig. 5 | $Be^9$ = 9.013<br>$O^{16}$ = 16.00 | |
| Secondary coolant | Potassium<br>K | 0.860 | Fig. 6 | K = 39.10 | Density as function *L* is also given in Fig. 6 |

tion, the UC will be in granule form, the expansion will be higher than that determined from sizeable samples (Ref. 8). The error in the density values at room temperature can be assumed to be 1%, and in the thermal expansion coefficients ± 10%. This uncertainty noticeably limits the accuracy of calculated volume fractions and atomic densities.

## B. *Dimensions and Volumes as Functions of Temperature*

Using the given values in Table 5 and Figs. 2, 4, 5 and 6 for the materials properties, the dimensions and volume changes as functions of temperature have been calculated. This has been done assuming that the central

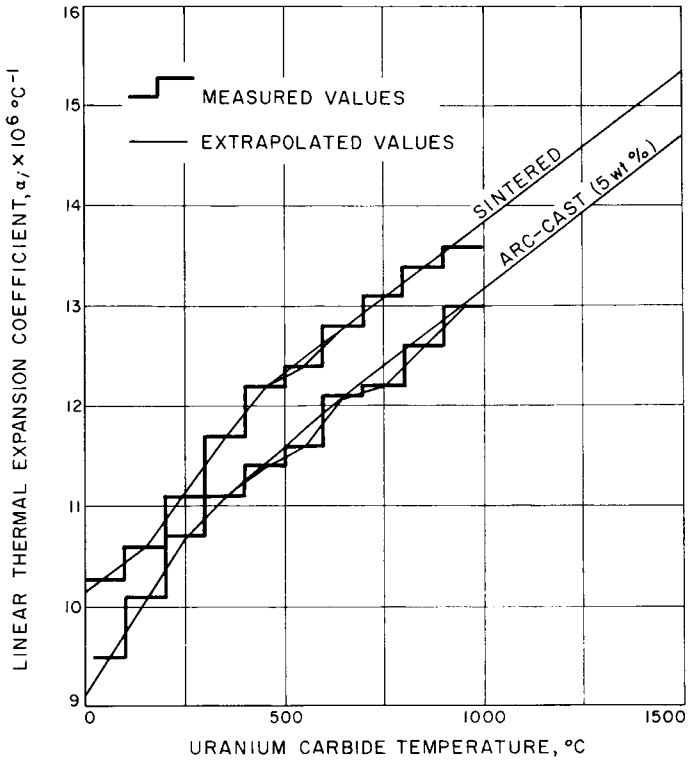


**Fig. 4. Linear thermal expansion coefficient for Uranium Carbide (Ref. 6)**

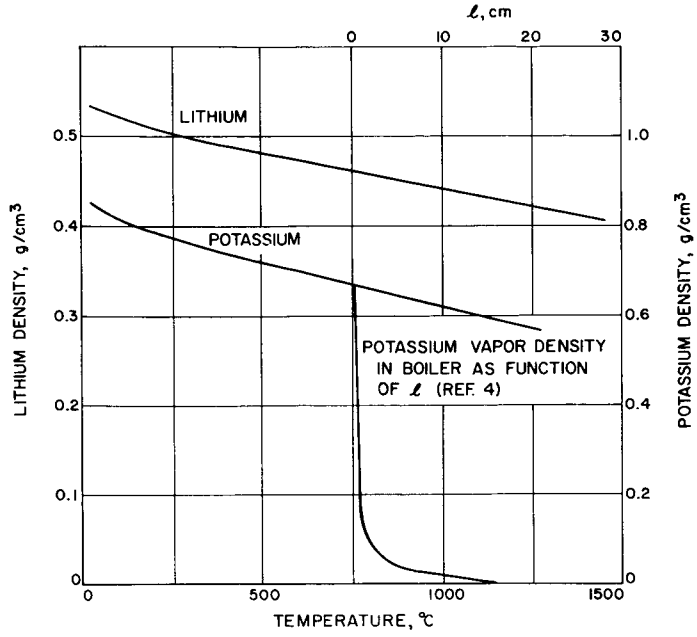


**Fig. 6. Lithium and Potassium density as a function of temperature (Ref. 7)**

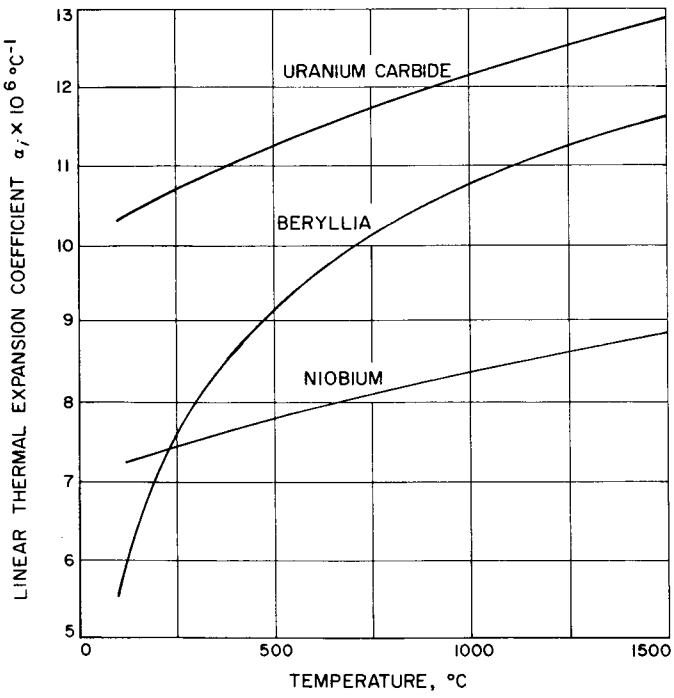


**Fig. 5. Linear thermal expansion coefficient $\alpha_i$ (20°C→T°C) for Uranium Carbide, Beryllium and Niobium**

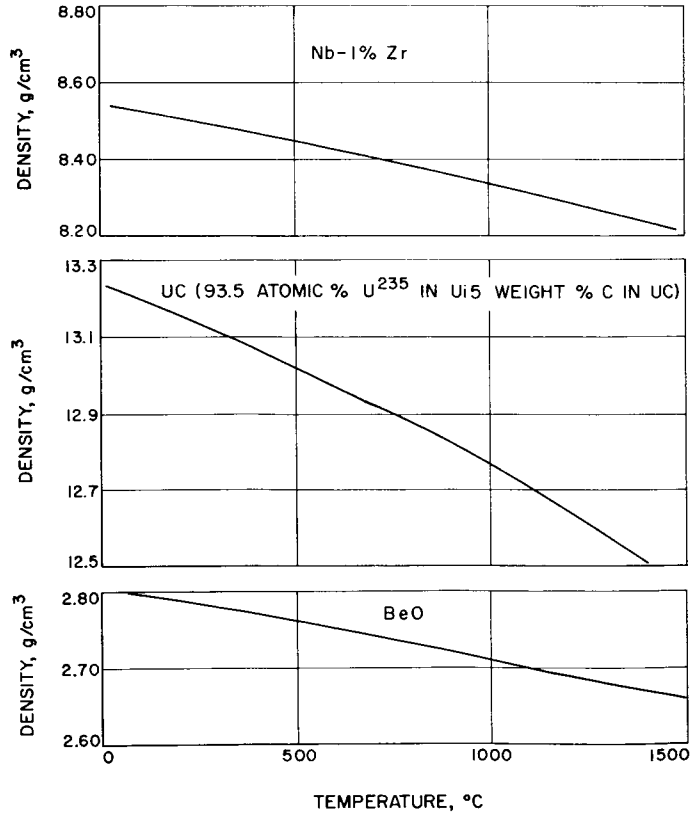


**Fig. 7. Density as a function of temperature for Nb-1% Zr; UC and BeO**

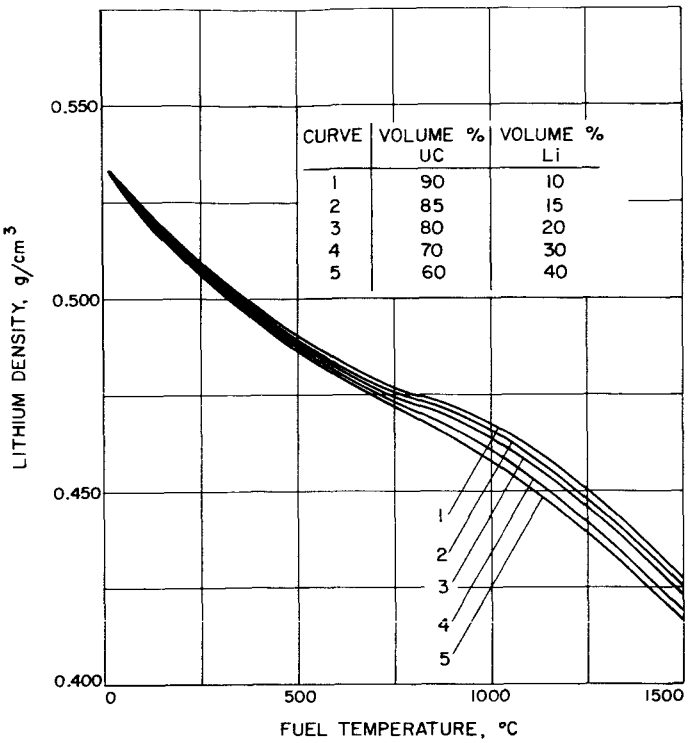


**Fig. 8. Average Li density in core as a function of fuel temperature and slurry concentration**

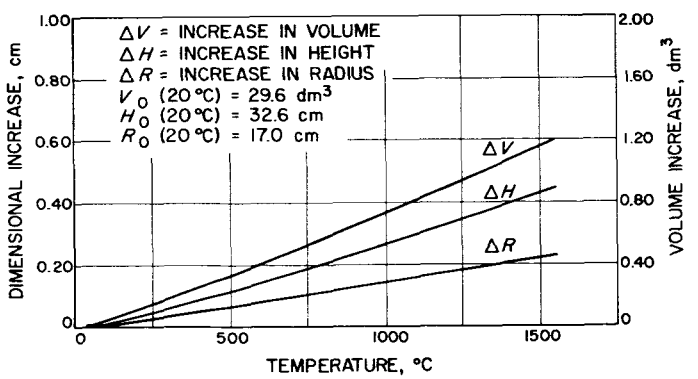


**Fig. 9. Increase in core dimensions and volume as a function of core vessel temperature**

diffusion wall and cavity have been replaced by 7 coolant pipes and fuel slurry. The influence of the central zones on reactivity is estimated with reference to this "homogenized" core in Section IV of this Report. Results are given in Figs. 7 to 10. The volume fractions remain practically constant as functions of temperature. Since the change is less than the uncertainty arising from the errors in the expansion coefficients, a constant relationship is assumed. The volume fractions in the homogenized radial coolant channel are 50 vol % Li and 50 vol % Nb-1% Zr. Corresponding values for the core vessel end plates are 25.9 vol % Li and 74.1 vol % Nb-1% Zr.

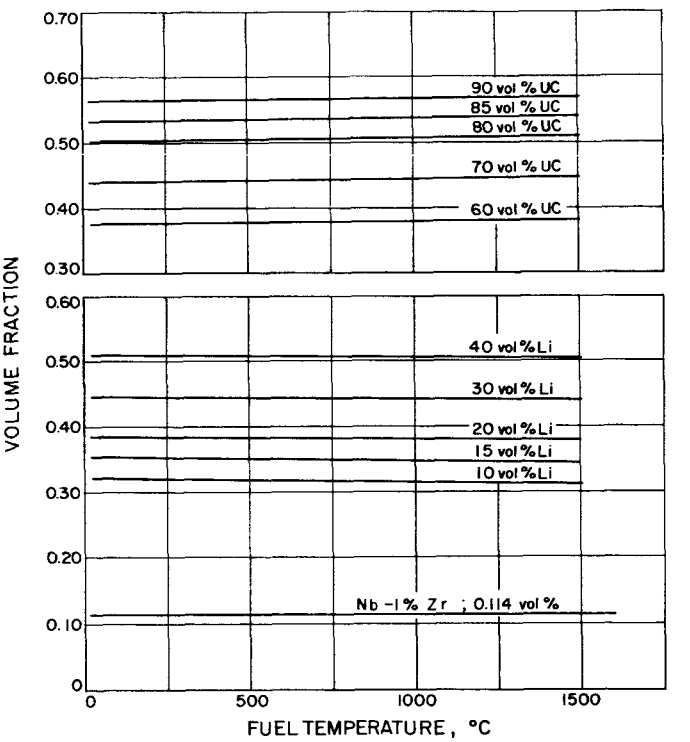


**Fig. 10. Volume fractions of UC, Li and Nb-1 % Zr as functions of fuel temperature and slurry concentration**

# III. CRITICALITY CALCULATIONS

Beginning with the given conceptual design, the objective is to investigate parameter influences as described in Section II. Given first are comments on some general aspects.

The reactor core size and materials are also determined by weight and heat transfer considerations, and are kept invariant in the analysis. Major changes in reactivity arise from changes in the fuel concentration and in the radial reflection, while changes in the axial reflection will have small impact. Judging from previous results (Ref. 1), the weight of the critical reactor remains approximately constant as the thickness of the BeO reflector varies. The task is therefore to optimize the radial reflectors to give enough reflector control and to keep the radial power generation shape factors within tolerable limits. Axially, it is also required that the power shape factors stay within acceptable values and that the boiler be "nuclearily" separated from the reactor so that any changes in the boiler operating conditions will give reactivity changes less than 1$. One would expect the axial BeO reflector at the coolant exit end to be of limited value mainly because of its ineffective shape and the coolant gap between it and the end plate.

These problems could possibly be alleviated by increasing the thickness of both end plates. However, the absolute axial leakage must also be determined with respect to the radial reflector worth required.

The needed reflector worth is mainly determined by the cold-to-hot temperature coefficients and fuel burn-up. Both factors warrant specialized investigation. Except for the delayed temperature coefficient, no attempt is made to include them here. The calculations are carried out for the clean reactor, and these suffice to show how any excess reactivity can be taken out of the reflectors.

Another question arises as to whether the reactor should be obtimized by adjusting the fuel slurry concentration while keeping the enrichment constant (or vice versa). One would expect concentration optimization to give minimum weight to the system, while the nuclear characteristics would favor the highest possible amount of $U^{238}$ in the core. However, the limits within which variations are possible are small, and many other pertinent considerations enter into this problem. In the calculations to follow, the slurry concentration is varied, and the enrichment is held at 93.5 at.% $U^{235}$ in U.

Two one-dimensional multigroup codes, *AIM*-6 (Ref. 9) and FORTRAN *SNG* (Ref. 10), were available for the calculations. The former code solves the neutron transport equation in the $P_1$-approximation; the latter uses the $S_n$-method. Because of the inherent limitations of these codes, simplifying assumptions must be made.

The *AIM*-6 code was used extensively in the production calculations, while the *SNG* code was used to check a few cases. The two-dimensional nonseparable problems here inhibit the full use of the latter code because of difficulties in correcting for the transverse leakage in the iterative flux-synthesis technique that must be employed. Both codes treat the anisotropy in the elastic scattering and slowing down collisions inadequately. However, a diagonal transport approximation in the *SNG*-problems gives generally a much smaller error than the $P_1$-approximation, and has been shown to give quite accurate results for $k_{eff}$ in unreflected fast reactors.

The error probability increases considerably for reflected reactors and systems containing light materials (Refs. 11 and 12). Attempts to improve the accuracy of the $P_1$-approximation using corrections derived from transport theory are hampered by ambiguities in the choice of definitions, and by the fact that "improvements" do not necessarily lead to greater accuracy. Specifically in the present application, for a given cross-section set, the choice of boundary conditions and definition of the diffusion coefficient critically influence the results.

In the approach taken here, *AIM*-6 and FORTRAN *SNG* calculations for simple one-dimensional cases are first compared, and a cross-section set is selected. The comparison serves merely as a guideline to establish probable error limits due to the computational method and to indicate the consistency of the *AIM*-6 results. Consequently, the absolute $k_{eff}$ value is not very accurate, but final adjustment can be achieved by changing the slurry concentration. The calculated $\delta k/k_{eff}$ remain independent enough of the slurry concentration for the present purposes.

A different approach was used making all calculations in spherical geometry with the *SNG* code to find $k_{eff}$ and estimating the critical mass in cylinder geometry using shape factors. This eliminated the difficulties mentioned for the application of the $P_1$-approximation. It was concluded that for the present purposes, the somewhat increased reliability of the results did not outweigh the practical advantages offered by the *AIM*-6 code. Also, for the fully reflected reactor, there were difficulties with the convergence in the *SNG* problems.

### A. The AIM-6 Code

The *AIM*-6 code (Ref. 9) solves the one-dimensional transport equation in the (inconsistent) $P_1$-approximation, i.e.,

$$-D^i \nabla^2 \Phi^i + \sum_t^i \Phi^i = x^i \sum_i \frac{(\nu\Sigma_f)^i \Phi^i}{k_{eff}} + \sum_{j=g}^{i-1} \sum_{s_1 j} \rightarrow i \, \Phi^j \tag{1}$$

where

$(B^2)^i$ = transverse buckling
$D^i$ = diffusion coefficient
$i, j$ = group indices
$k_{eff}$ = the effective multiplication constant for the system
$t^i$ = ratio of poison cross-section in group $i$ to thermal poison cross-section
$x^i$ = integral of the fission spectrum over the lethargy range presented by group $i$
$(\nu\Sigma_f)^i$ = average number of neutrons produced times the fission cross-section
$\Sigma_a^i$ = absorption cross-section
$\Sigma_p^{th}$ = poison cross-section in thermal group
$\Sigma_{s_1} i \rightarrow j$ = transfer cross-section from group $i$ to group $j$
$\Sigma_t^i$ = total removal cross-section $= D^i (B^2)^i + \Sigma_a^i + t^i \Sigma_p^{th} + \sum_{j=i+1}^{1} \Sigma_{s_1} i \rightarrow j$
$\Phi^i$ = neutron flux

The use of the *AIM*-6 code as such is straightforward. To facilitate the calculations without resorting to lengthy specialized derivations, it was decided to indiscriminately use the extrapolation length option of the code. This applies formulas derived by Cohen (Ref. 13). The code calculates $\omega$ for the expression

$$\left| \phi^i(r) + \omega^i \frac{d\phi^i}{dr} \right|_R = 0 \tag{2}$$

putting $\omega^i = 3D^i \times 0.710446$ (plane geometry)

$$= 3D^i \frac{0.710446}{1 + 0.710446\, 3LD^i/2r_n} \tag{3}$$

$$\begin{pmatrix} L = 1 \text{ in cylindrical geometry} \\ L = 2 \text{ in spherical geometry} \end{pmatrix}$$

Cohen's formulas can most safely be used when the boundary region has relatively weak capture and is several mean free paths thick—conditions most closely met for the fully reflected case. In the above formulas, the diffusion coefficient is defined as

$$D^i = \left[3\left(\sum_{tot}^i - \mu^i \Sigma_s i\right)\right]^{-1} = 1/3\,\Sigma_{tr} \tag{4}$$

and is calculated by the code. Optionally, for expression (1), $D^i$ can be defined as

$$D^i = \left[3\,\Sigma_{tr}^i \left(1 - 2\Sigma_a^i/5\Sigma_{tr}^i\right)^2\right]^{-1} \tag{5}$$

a formula somewhat different from the one usually applied in asymptotic reactor theory;

$$D^i = \Sigma_a^i/(\kappa^2)^i = \left[3\Sigma_{tot}^i (1 - \mu^i)(1 - 2\Sigma_a^i/5\,\Sigma_{tot}^i)^2\right]^{-1} \tag{6}$$

An investigation showed that for a given cross-section set the computed $k_{eff}$ was higher when Eq. (4) was used instead of Eq. (5) for $D^i$. This was to be expected. There was also a closer agreement with results from reference *SNG* calculations to be discussed next. However, results in both cases stayed within the error limit for the *SNG* results, taken to be $< +5\%$. Since Eq. (5) attempts to account for the absorption effect, it was used extensively.

For the two-dimensional calculations, flux synthesis techniques were used. The calculations were simplified by iterating toward the common $k_{eff}$ using group, region and energy independent transverse bucklings. Since the extrapolation length is group dependent, according to Eq. (3) this introduces an inconsistency. It was found that the difference in results from the consistent and inconsistent treatment gives an error in $\delta k/k_{eff}$ of as much as 10%. The constant transverse bucklings were deduced for the unreflected and reflected reference reactor given in Fig. 2.

The diffusion coefficient for the annular void region between the reactor vessel and reflector could be calculated using formulas given in Refs. 14 and 15. The diffusion coefficient is here an energy independent geometry factor. The given expressions assume zero transverse leakage, and the leakage cannot be accounted for using

$D_{void} \cdot B^2_{axial}$. Since the gap is narrow and the calculated $D_{void} = 44.6$ cm is high, the gap region has been omitted in the calculations. It is important to keep the gap as narrow as possible since the reflector worth rapidly decreases with increased gap width.

### B. Multigroup Cross-Sections

A number of multigroup cross-section sets for fast reactor calculations have been published. The accuracy of the predicted $k_{eff}$ and the sensitivity to uncertainties in nuclear data are dependent on the reactor to which the sets are applied. Attempts to produce universal sets by suitably adjusting high energy data have been only partially successful. Most adjustments have been made using the $S_n$-method in the neutronics calculations. These same sets, when used in $P_1$ calculations, generally give lower $k_{eff}$ values for a given smaller fast reactor.

The other approach (adjusting a cross-section set to $P_1$ neutronics calculations) has also been tried. The shortcomings of the $P_1$-approximation make this a less satisfactory method.

Using the boundary conditions and diffusion coefficients as provided by the *AIM*-6 code for very small, fast systems, it is impossible to get reasonable agreement between *AIM*-6 and *SNG* results utilizing the same cross-sections. To get the correct critical mass with the former code, artificially high $(\nu\Sigma_f)^i$ and $\Sigma^i_{tr}$ cross-sections must be postulated. However, for the present system, it was found that the discrepancy for $k_{eff}$ stayed within 5%, the *SNG* code giving the higher values. The reference calculations were carried out with the reactor system taken as infinite slabs and cylinders. From results for the accuracy of the transport approximation in $Sn$-method calculations (Refs. 14, 15), the *SNG* $k_{eff}$ values have a positive error $< 5\%$ for a given cross-section set.

A modified 16-group set based on the 16-group (deck 3W-383) and 18-group (deck 3W-391) sets optionally included in the *AIM*-6 write-up was used. For elements $U^{235}$ and $U^{238}$, the cross-sections in groups 1 through 6 were taken from the 18-group set replacing corresponding 16-group data. The newer data were then included in the basic 16-group set. The Nb inelastic cross-sections were taken from Zr data, but no attempts were made to correct for this or any of the cross-sections for the other elements. A few calculations with the original 16-group set were also made. As expected, the $k_{eff}$ values were lower, but the computed $\delta k/k_{eff}$ remained relatively unaffected. Naturally, for the reference *SNG* calculations, the cross-section sets were suitably rearranged.

For high temperature calculations, the basic cross-sections should be changed due to Doppler broadening of the resonances. A full investigation of this effect requires an elaborate analysis, which as yet has not been undertaken. The same basic cross-section set was used for all temperatures. From a preliminary investigation, it can be concluded that the prompt temperature coefficient for the fuel due to the Doppler effect is positive and small, $\approx 1 \times 10^{-6}\ \delta k/°C$. If natural Li instead of $Li^7$ is used as primary coolant and fuel slurry solvent, a positive coefficient arises from the $1/v$ part of the absorption cross-section; but there is also a negative contribution from the 0.28 Mev resonance peak. The spectral distribution in the reactor studied here enhances the importance of this peak, and there are few neutrons in groups below 55 Kev (groups 9 to 16) also when the reactor is radially fully reflected (see Section IV D).

A strong negative temperature coefficient comes from the expansion of the core as a whole. Since the relative importance of the positive and negative contributions during a power excursion is also dependent on the heat conduction characteristics, the overall behavior can only be determined after detailed analysis. However, tentatively and because natural Li introduces other desirable features (to be discussed later), the calculations are carried out for this material.

### C. Some Basic Criticality Calculations

As a basis for the more detailed parameter studies, the general characteristics of the reactor system are first investigated. As reference reactor, the simplified version given in Fig. 2 is taken without the axial regions outside the core vessel end plates and the central diffusion plug. Natural Li is chosen as primary coolant and fuel slurry solvent. The calculational method and cross-sections are as described in Section IV. The temperature is 68°F.

It is instructive to study the system separately in the axial and radial directions in terms of the total transverse leakage. Figure 11 shows $k_{eff}$ as a function of the transverse buckling and slurry concentration. The *operating* point has been marked. The line crossing over the results for the radial calculations shows the shift in operating point when the slurry concentration is changed or when one goes from the unreflected to the reflected case. Actually, these changes follow separate paths, but it was found that they nearly overlap and stay within the

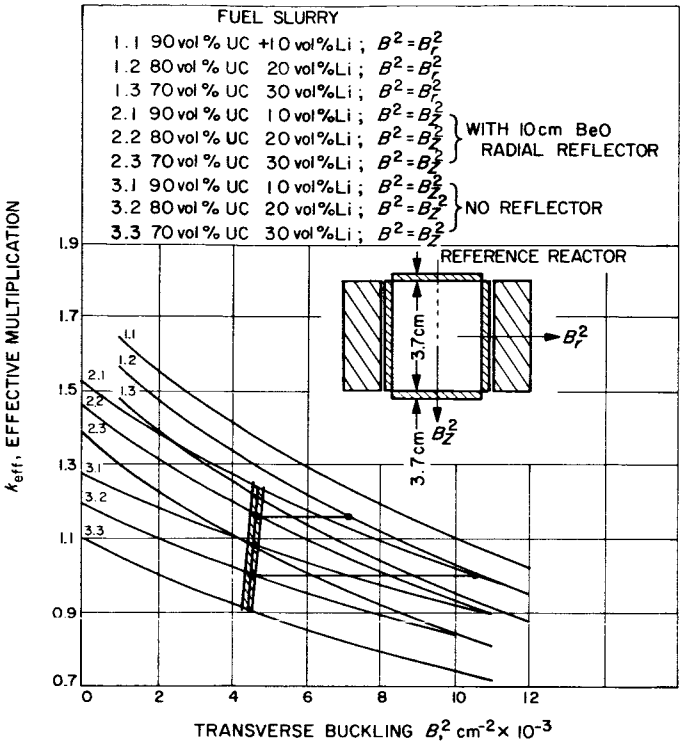


**Fig. 11. The effective multiplication as a function of the transverse leakage and fuel slurry concentration**

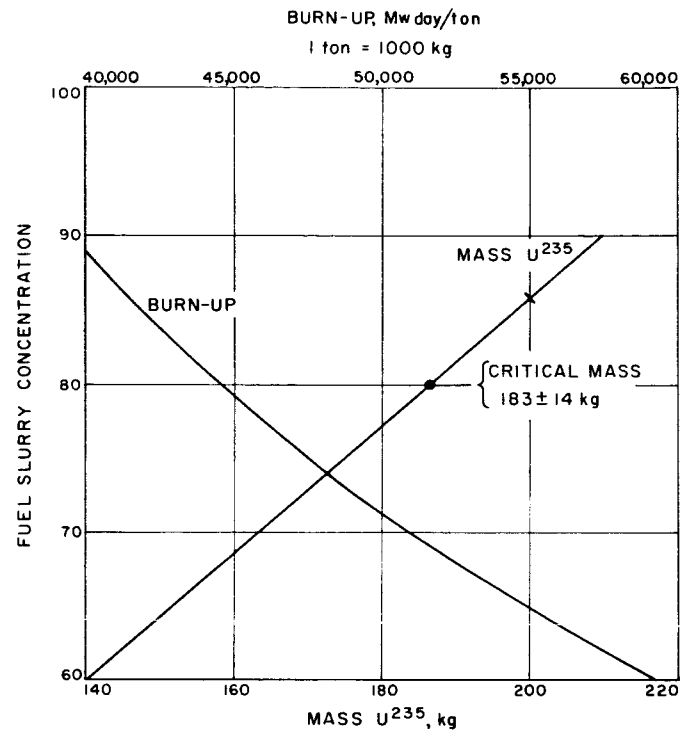


**Fig. 12. Mass $U^{235}$ and required burnup as a function of fuel slurry concentration**

approximate field of error also indicated in Fig. 11. One can conclude that the reference reactor is nearly separable. Because of the symmetry requirements, both end plates have the same thickness of 3.7 cm, which represents the design thickness on the boiler side. The leakage through the coolant exit site is therefore underestimated as compared to the actual design and the $k_{eff}$ is overestimated nearly 1%.

The computed critical slurry concentration for the unreflected reactor is 80 ± 6 vol % UC applying the estimated error in $k_{eff}$, ±5%. The critical mass becomes 183 ± 14 kg $U^{235}$ (Fig. 12), corresponding to 45,000 ± 3000, Mwday/ton required burnup (i.e., for 10 Mw thermal effect and 20,000 hr at full power). A total of 9.7 kg $U^{235}$ will be consumed. Of this amount, 0.7 kg represents parasitic capture in $U^{235}$.

The contribution to the power output from fissions in $U^{238}$ is about 1%, and about 0.1% from thermal fissions in $U^{235}$ when the reactor is fully reflected.

The required burnup is rather high and cracking and swelling of the UC to a considerable extent can be expected. Very few data for these effects exist for UC in the contemplated burnup region. Obviously, most measurements have been taken for massive UC, and few for slurries. A conservative guess for the present case would be 3 vol % swelling, with a corresponding amount of Li being squeezed out from the slurry (Ref. 6). For slurries, nothing is known about the possible agglomeration of the UC particles. As indicated earlier, the calculations here are for the clean, fresh reactor, and no attempts are made to study in a general way the mentioned effects.

# IV. RESULTS OF PARAMETER STUDIES

Except for the calculation of the delayed temperature coefficient, all parameter studies have been made at room temperature (68°F). As a result, an upper bound in the computed relative quantities is determined. From the reference calculations it can be concluded that the use of a constant group, region, and energy, independent transverse buckling introduces an error $< \pm 10\%$ in $\delta k_{eff}/k_{eff}$ when the geometry is varied in the computational direction. For the present purposes, this error justifies the simplified approach and does not introduce intolerable errors for other computed quantities. Their probable accuracy is mentioned separately.

## A. Choice of Natural Li or $Li^7$ as primary coolant and Slurry Liquid

Under Section III, some possible implications of the use of natural Li instead of $Li^7$ were mentioned. Furthermore, the penalty in fuel inventory is insignificant. Within the contemplated slurry concentration region $\delta k/k_{eff}$ $Li^7 \rightarrow Li$ is $-2\%$ for the unreflected case and $-3.5\%$ for the reflected case. The savings in fuel inventory would then be nearly 2 vol % UC, and a small decrease in reflector worth is achieved. The latter is, however, more than compensated through the decrease in the total delayed (negative) temperature coefficient when heating the reactor to operating temperature.

Other advantages offered by the use of natural Li include depression of the thermal and epithermal neutron fluxes and depression of the power peaking at the radial edge. The burnup of $Li^6$ through the $Li^6$ $(n_1\alpha)H^3$ reaction compensates for fission product poisoning. About 4% of all absorptions in the core produce $H^3$, an element which possibly can introduce undesired chemical reactions.

Taking into account the prompt fuel expansion during a power excursion, one would deduce that $Li^7$ should be chosen as slurry liquid and $Li^6 + Li^7$ as primary coolant. Then, the lithium squeezed out from the slurry would not be felt as a positive contribution to the prompt temperature coefficient. Pending further investigations, natural Li is taken as the basic material in all calculations.

## B. Radial and Axial Power Shape Factors and Power Generation Distributions

In Fig. 13, the axial and radial (peak power/average power) ratios are shown as functions of the transverse buckling. They apply to the same reference reactor shown in Fig. 11. Constructional changes in the regions outside the end plates introduce less than 0.5% variation in the shape factors. Increasing or decreasing the end plate thicknesses to either extreme, while keeping the other axial regions as in the reactor of Fig. 2 would give a 5% change. Axially, only insignificant improvements in the shape factors can be made with the given design. However, the arrived at value, $\sim$ 1.2, can be regarded as satisfactory.

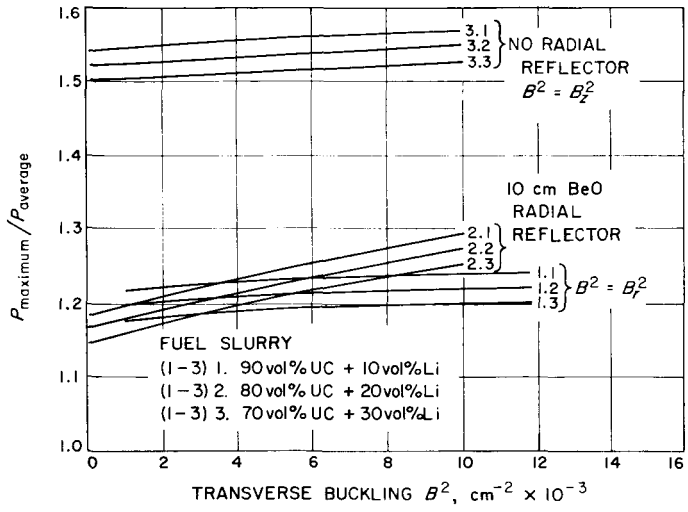


**Fig. 13. Peak power/average power ratios as functions of transverse buckling and fuel slurry concentration**

In the radial direction, the difference between the reflected and unreflected case is significant and suggests some measures to minimize the change over the reactor lifetime. In Section C, a modification of the present reflector design is presented that automatically improves the radial shape factor for the clean, and hot reactor. The possibility of further improvements by dispersing a suitable poison and compensating by increasing the radial reflection will be investigated. Such a poison should have strong high-energy resonance absorption. Perhaps manipulations with the $Li^6$ content in the core will produce this absorption. Also, the effects of dispersing an absorber in the uranium-carbide will be evaluated.

In Fig. 14, the power generation ratios vs core radius and height are given. The curve for the case of no radial reflector corresponds to the clean, critical reactor. The curve for the reflected case, which corresponds to a

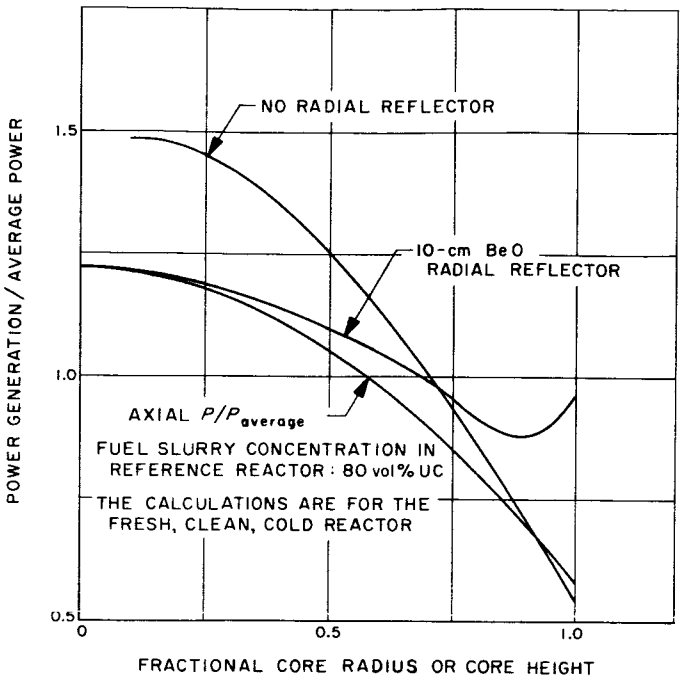


**Fig. 14. Power generation ratios vs core radius and core height**

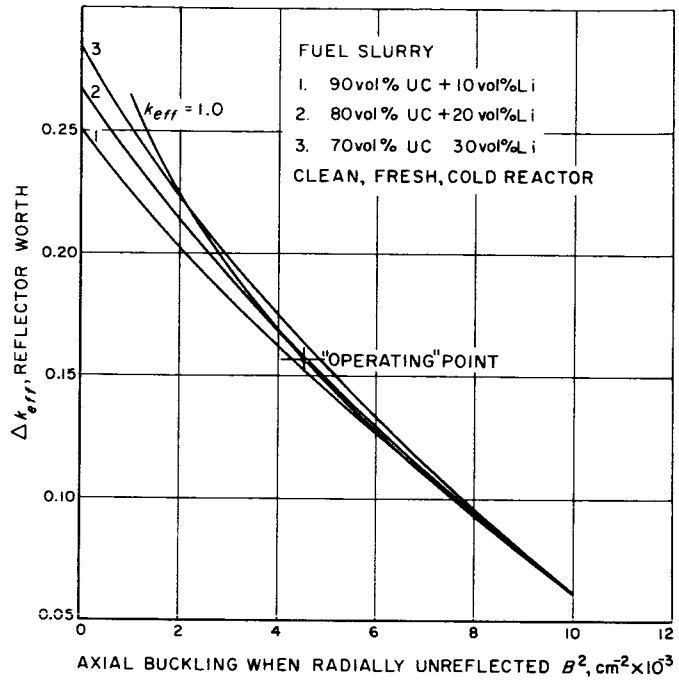


**Fig. 15. Reflector worth as a function of the axial buckling and fuel slurry concentration**

supercritical reactor, gives only a hint of what the distribution will look like radially at the end of life. The axial distribution will also flatten with time, but not as much as the radial distribution.

## C. *Reflector Worth*

The needed excess reactivity in the reflectors is mainly determined by the following factors:

1. Cold-to-hot temperature coefficient (expansion)
2. Fuel burnup
3. Cold shut-down level

Of lesser importance when quantitatively assessing the required reflector worth are:

4. The Doppler effect
5. The fission products
6. Burnup of absorbing nuclei in constructional material and coolant

Computed results indicate that (1) requires nearly 6.5% $\delta k/k_{eff}$ and that (2) requires nearly 5% $\delta k/k_{eff}$. Item (3) above depends largely on how the reactor system is assembled and the general safety policy. Tentatively, 3% $\delta k/k_{eff}$ can be put here. Items (4–6) give both positive and negative contributions, the exact balance of which at this time cannot be determined. The effectiveness of the central diffusion wall and the exact slurry and coolant composition critically affect these values. A rough estimate of $-1\%$ $\delta k/k_{eff}$ is assumed. In total, about 15% $\delta k/k_{eff}$ must be taken out with the reflectors.

Figure 15 shows the calculated reflector worth for the reference bare reactor. Axial regions outside the end plates change the results insignificantly, but a change in the thickness of the end plates has a considerable effect. Increasing the reflector thickness from 10 cm to 15 cm gives only a 10% increase in the $\delta k/k_{eff}$ values at the "operating" point. At this point, nearly 15% $\delta k/k_{eff}$ is available, which is the same amount estimated as needed. In order to increase the reflector worth, one can increase the end plate thickness. Thus, 8-cm-thick end plates give 20% $\delta k/k_{eff}$ for a 10-cm-thick BeO reflector. The fuel slurry concentration must then be decreased from 80 vol % UC to 75 vol % UC. A detailed study will determine the

cooling requirements of the reflectors, and the factors above point out the possibilities of decreasing the reflector thickness if necessary while retaining 15% $\delta k/k_{eff}$. However, increasing the end plate thickness beyond 8 cm will give insignificant improvements.

There are several advantages to splitting the radial reflectors as shown schematically in Fig. 16. The 10-cm-thick BeO reflectors are split lengthwise into two concentric 3-cm- and 7-cm-thick parts. The inner part compensates for the large negative temperature coefficient that arises when the reactor is heated to operating temperature, but only so much that the reactor is slightly subcritical. If nuclear preheating of the core is employed, the inner reflectors are used for start-up. Criticality and control is then maintained with the outer reflectors. The concentric parts are connected to the same feed shaft so that the outer reflectors begin to move when the inner ones are fully inserted. The described design maintains essentially the original method of reflector control, but improves the control characteristics and radial power generation distribution for the clean reactor. Refinements in the form of shaping and varying the material lengthwise in the outer reflectors will be made to optimize the reflector performance.

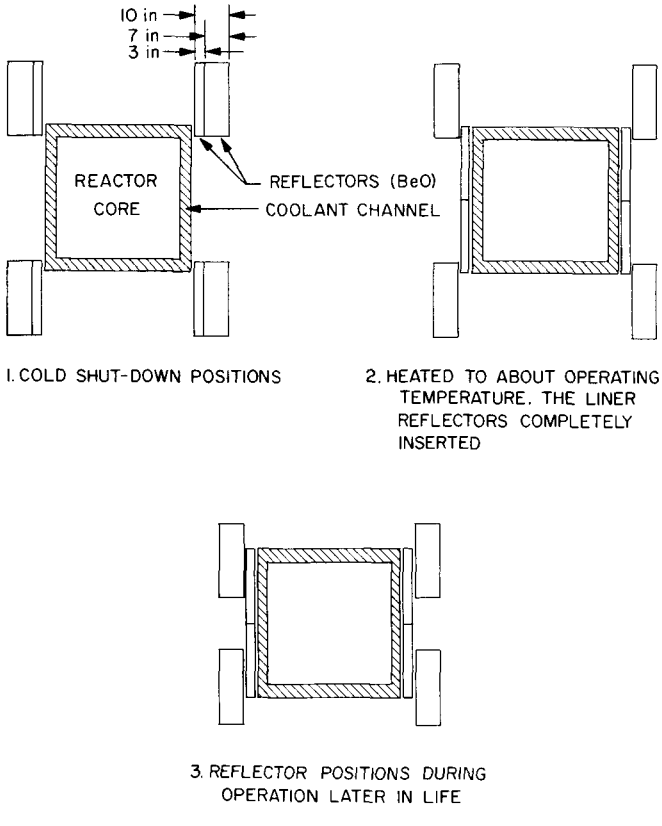


**Fig. 16. Proposed reflector construction to improve power shape factors and control characteristics**

## D. Neutron Spectrum Distribution

Neutron flux values in the reactor core for each group normalized to 1w thermal power are given in Table 6. The iterative flux synthesis technique used in the calculations did not produce unique values (although the $k_{eff}$ values converged), and the error at the core edges is estimated to about $\pm$ 10% for the first 10 groups, i.e., apart from other error sources. At midcore, the numerical accuracy is $\pm$ 5%. To simulate the reactor at the end of its life, the fluxes in the fully reflected core were computed for a 5 vol % lower UC content, and the leakage increased to give $k_{eff} \sim 1.0$. Of course, only a rough estimate of the flux changes can be obtained this way.

The median flux energy for the radially unreflected clean and cold reactor is 0.74 Mev, and for the calculated reflected case, 0.62 Mev. The reactor is very fast and the effective delayed neutron fraction can be expected to be $\beta_{eff} \sim 0.007$. A reactivity insertion of $\beta k/k_{eff} = 0.005$ ($= 71¢$) would thus give a stable reactor period of $T_p = 1$ sec. Correspondingly, for $T_p = 10$ sec, $\delta k/k_{eff} = 0.0025$ ($= 36¢$).

## E. Influence of Constructional Components

As pointed out earlier, it is important to know the influence on reactivity of the axial regions outside the reactor core.

In Fig. 17, the results of parameter studies for these regions are given. The results for each case refer to the axially symmetric reactor, i.e., in the calculations, the midplane (Z = 0) was taken as the reference plane. Since the material densities were chosen for room temperature, the boiler is considered completely filled with potassium, lithium and coolant piping, and the axial BeO reflector is of uniform thickness, the $\delta k/k_{eff}$ values represent upper bounds. In reality, the numerical values will be lower than those given. This is true for the radially fully reflected reactor as well.

It can be seen from Fig. 17 that the boiler and axial reflector insignificantly affect the reactivity. Thus, the axial reflector will be omitted, and any conceivable

**Table 6. Neutron flux in reactor core. Normalized to 1w thermal power**

| Energy group, $i$ | Lower energy limit in group $i$, Mev | Neutron flux in core | | | $n \times cm^{-2}sec^{-1}$ | | |
|---|---|---|---|---|---|---|---|
| | | No radial reflector 80 vol % UC + 20 vol % Li | | | 10 cm BeO radial reflector 75 vol % UC + 25 vol % Li | | |
| | | Midcore | Radial edge (midplane) | Axial edge (on axis) | Midcore | Radial edge (midplane) | Axial edge (on axis) |
| 1 | $3.0 \times 10^{0}$ | $4.2 \times 10^{6}$ | $1.6 \times 10^{6}$ | $1.9 \times 10^{6}$ | $3.7 \times 10^{6}$ | $1.7 \times 10^{6}$ | $1.7 \times 10^{6}$ |
| 2 | $1.4 \times 10^{0}$ | $1.0 \times 10^{7}$ | $3.8 \times 10^{6}$ | $4.8 \times 10^{6}$ | $8.6 \times 10^{6}$ | $4.4 \times 10^{6}$ | $4.2 \times 10^{6}$ |
| 3 | $9.0 \times 10^{-1}$ | $6.1 \times 10^{6}$ | $2.3 \times 10^{6}$ | $3.0 \times 10^{6}$ | $5.2 \times 10^{6}$ | $2.7 \times 10^{6}$ | $2.6 \times 10^{6}$ |
| 4 | $4.0 \times 10^{-1}$ | $1.3 \times 10^{7}$ | $4.8 \times 10^{6}$ | $6.4 \times 10^{6}$ | $1.1 \times 10^{7}$ | $6.0 \times 10^{6}$ | $5.7 \times 10^{6}$ |
| 5 | $1.0 \times 10^{-1}$ | $1.1 \times 10^{7}$ | $3.6 \times 10^{6}$ | $4.9 \times 10^{6}$ | $8.9 \times 10^{6}$ | $5.3 \times 10^{6}$ | $4.3 \times 10^{6}$ |
| 6 | $1.7 \times 10^{-2}$ | $3.5 \times 10^{6}$ | $1.2 \times 10^{6}$ | $1.6 \times 10^{6}$ | $3.0 \times 10^{6}$ | $2.8 \times 10^{6}$ | $1.4 \times 10^{6}$ |
| 7 | $3.0 \times 10^{-3}$ | $3.1 \times 10^{5}$ | $1.1 \times 10^{5}$ | $1.5 \times 10^{5}$ | $2.9 \times 10^{5}$ | $8.0 \times 10^{5}$ | $1.4 \times 10^{5}$ |
| 8 | $5.5 \times 10^{-4}$ | $2.9 \times 10^{4}$ | $9.0 \times 10^{3}$ | $1.1 \times 10^{4}$ | $2.6 \times 10^{4}$ | $2.7 \times 10^{5}$ | $1.1 \times 10^{4}$ |
| 9 | $1.0 \times 10^{-4}$ | $7.0 \times 10^{2}$ | $2.6 \times 10^{2}$ | $2.9 \times 10^{2}$ | $6.6 \times 10^{2}$ | $9.4 \times 10^{4}$ | $2.8 \times 10^{2}$ |
| 10 | $3.0 \times 10^{-5}$ | $9.0 \times 10^{0}$ | $5.0 \times 10^{0}$ | $6.2 \times 10^{0}$ | $7.7 \times 10^{0}$ | $4.8 \times 10^{4}$ | $5.5 \times 10^{0}$ |
| 11 | $1.0 \times 10^{-5}$ | — | — | — | — | $2.4 \times 10^{4}$ | — |
| 12 | $3.0 \times 10^{-6}$ | — | — | — | — | $1.6 \times 10^{4}$ | — |
| 13 | $1.0 \times 10^{-6}$ | — | — | — | — | $8.1 \times 10^{3}$ | — |
| 14 | $4.0 \times 10^{-7}$ | — | — | — | — | $3.2 \times 10^{3}$ | — |
| 15 | $1.0 \times 10^{-7}$ | — | — | — | — | $1.3 \times 10^{3}$ | — |
| 16 | Thermal | — | — | — | — | $1.3 \times 10^{2}$ | — |
| Average fission energy, Mev | | 0.72 | 0.77 | 0.72 | 0.67 | 0.26 | 0.67 |
| Average absorption energy, Mev | | 0.55 | 0.60 | 0.56 | 0.51 | 0.13 | 0.53 |
| Average flux energy, Mev | | 0.73 | 0.76 | 0.72 | 0.70 | 0.58 | 0.70 |
| Core characteristics | | $k_{eff} = 1.0$; $B_r^2 = 0.0108$ cm$^{-2}$ $B_z^2 = 0.0045$ cm$^{-2}$ | | | $k_{eff} = 1.0$; $B_r^2 = 0.008$ cm$^{-2}$ $B_z^2 = 0.01$ cm$^{-2}$ | | |

change in the potassium level does not cause prompt criticality. Also, the stable period will be of sufficient length (magnitude of 10 sec). The thickness of the end plates affects the reactor physical properties significantly and balances the reflector thickness and fuel concentration (discussed earlier). Theoretically, it would be advantageous to make the end plates of the same thickness at both ends. However, a difference such as that on the conceptual design seems insignificant from a practical point of view.

The influence of the central diffusion wall and cavity was calculated with reference to the homogeneous reactor. With the given dimensions and materials, $\delta k/k_{eff}$ equaled $-0.5\%$, a plausible value.

## F. Temperature Coefficients

The total delayed temperature coefficient (not including the Doppler effect) was calculated for the homogenized core using the material constants derived in Section II. The calculational technique was the same as described earlier, and the reactor of Fig. 11 without radial reflector and with 80 vol % UC fuel slurry concentration was taken as reference reactor. The results are shown in Fig. 18. The change in $k_{eff}$ is practically linear over the whole temperature range, giving a constant differential temperature coefficient. Judging from the results in the previous section, the influences of the axial regions outside the end plates changes the values in Fig. 18 less than 5%, assuming dimensions as in the conceptual design and the system completely filled with primary and secondary coolant.

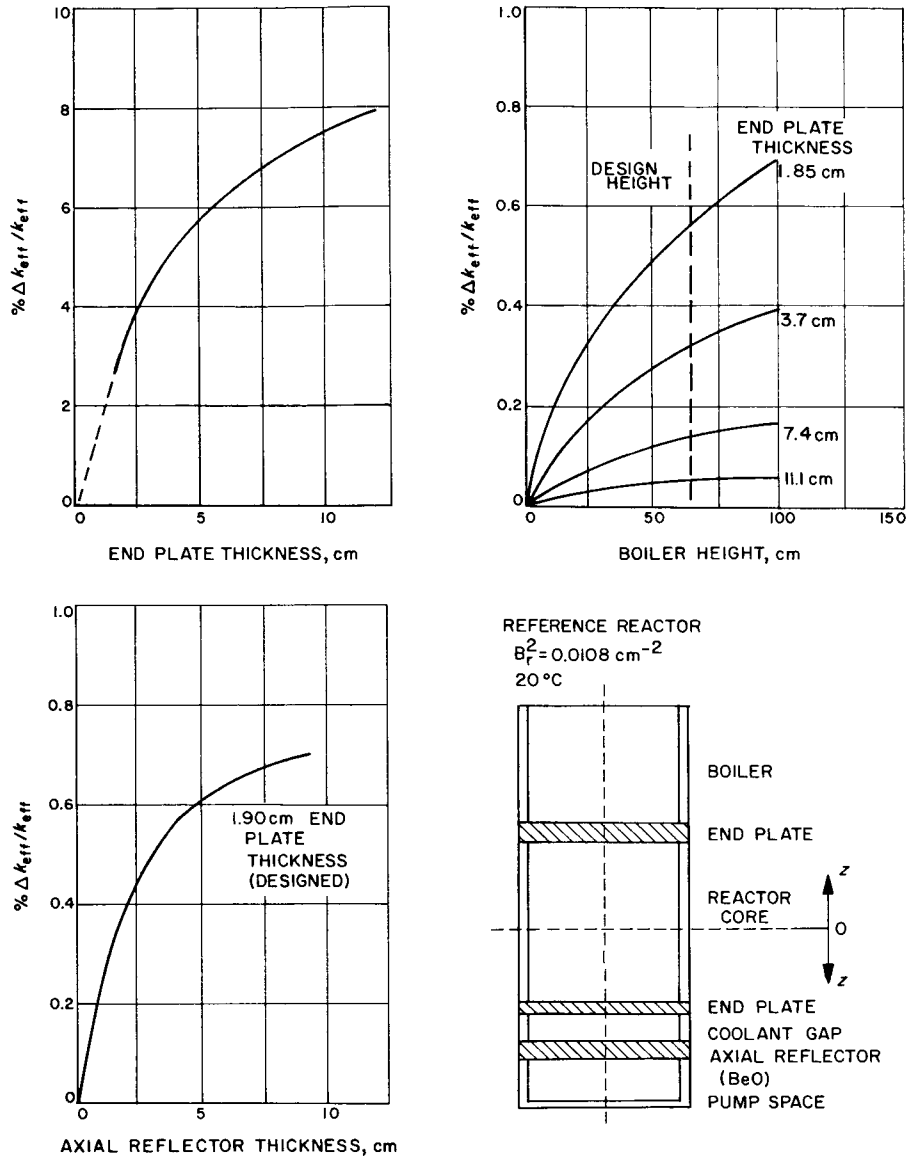


**Fig. 17. Reactivity changes vs thickness of axial structural components**

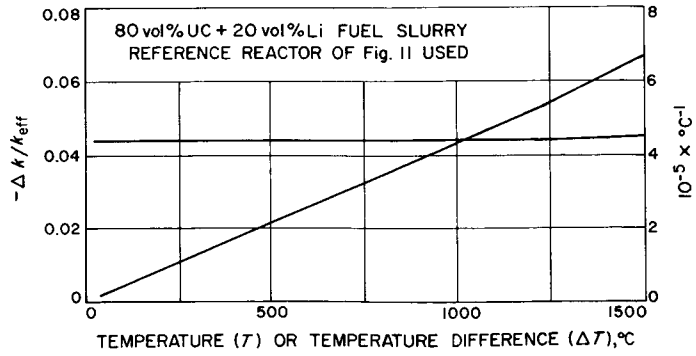


**Fig. 18. Total and differential delayed temperature coefficients**

# V. CONCLUSION

The results of the calculations indicate that the reactor concept under study has definite nuclear feasibility. Many details have not yet been resolved and the evaluations were approximate; but the design holds enough versatility to allow corrections without major modifications. One of the major problems remains the accurate determination of the prompt and delayed temperature coefficients, especially for the case of accidental prompt criticality. Other potential hazardous situations, such as loss of the primary coolant, must also be evaluated.

It has been shown that the axial BeO reflector should be omitted and that the boiler is well separated, in a nuclear sense, from the reactor core.

The modified radial reflector construction will bring about considerable improvements. The coolant channel between the core and the radial reflector shadows this reflector to some extent, but also prevents thermalized neutrons from returning to the core and power peaking at the core edge. In the design work, every effort will be made to keep the channel and the gap between the core and the reflector as thin as possible. If the axial reflection is improved, the radial BeO reflector can be a few cm thinner. The best practical way to improve the axial reflection without increasing the core height seems to be by increasing the thicknesses of the end plates. Finally, Table 7 lists some of the more important reactor characteristics which have been gathered.

**Table 7. Reactor physics properties for reactor in Fig. 2**

| Item | Characteristic | Approximate absolute error | Remarks |
|---|---|---|---|
| Critical mass | 183 kg, $U^{235}$<br>80 vol % UC + 20 vol % Li | ±14 kg<br>±6, vol % UC | No radial reflector<br>Beginning of life |
| Required Burnup | 9.7 kg $U^{235}$<br>45,000 Mwday/ton | ±3000 | 20,000 hr at 10 Mw<br>0.7 kg capture in $U^{235}$ |
| Fissions in $U^{238}$ | 1% of power output | | |
| Thermal fissions in $U^{235}$ | 0<br>0.1% | | No radial reflector<br>With 10 cm BeO reflector |
| Power generation | $F_{axial} = 1.2$<br>$F_{radial} = 1.5 \rightarrow 1.2$ | ±0.05<br>±0.1 | <br>Beginning to end of life |
| Reflector worth | +15% $\delta k/k_{eff}$ | ±2 | 10 cm BeO reflector |
| Median flux energy | 0.74 Mev<br>0.62 Mev | ±0.03<br>±0.03 | No radial reflector<br>With 10 cm BeO reflector |
| Temperature coefficients | −0.065 $\delta k/k_{eff}$<br>$-4.4 \cdot 10^{-5}$°C$^{-1}$ | ±0.007<br>$\pm 5.10^{-6}$ | Heating from 20°C to 1500°C<br>Differential |
| Control requirements | 6.5% $\delta k/k_{eff}$<br>5% $\delta k/k_{eff}$<br>3% $\delta k/k_{eff}$ | ±0.7<br>±0.5 | Heating to operating temperature<br>Fuel burnup<br>Others (estimated) |

## REFERENCES


1. Allen, L. S., *A Parameter Survey of Criticality-Limited Fast Reactors Employing Uranium Fluoride Fuels,* Technical Report No. 32-198, Jet Propulsion Laboratory, March 15, 1962.
2. Davis, J. P., *A Nuclear Reactor Concept for Electric Propulsion Application,* Technical Report No. 32-385, Jet Propulsion Laboratory, March 4, 1963.
3. Beale, R. J., *Systems Engineering of a Nuclear-Electric Spacecraft,* Technical Report No. 32-158, Jet Propulsion Laboratory, October 31, 1961.
4. Davis, J. P., Private Communication.
5. Kikin, G., Private Communication
6. Strasser, A., "Uranium Carbide as Fuel. A Review of Current Knowledge," *Nuclear Engineering,* August, 1960.
7. Etherington, H., Editor, "Nuclear Engineering Handbook," McGraw-Hill, 1958.
8. Phillips, W., Private Communication.
9. Flatt, H. P., and Baller, D. C., The *AIM*-6 Code, NAA, Program Description, January, 1961.
10. Lemke, B., Fortran *SNG* Code, *NAA* Program Description, July 28, 1959.
11. Pendlebury, E. D., and Underhill, L. H., "The Validity of the Transport Approximation in Critical-Size and Reactivity Calculations," *Proceedings of the Seminar on the Physics of Fast and Intermediate Reactors,* II, *SM*18/21, *IAEA,* Vienna, Austria, 1962.
12. Joanou, G. D., and Halim Kazi, A., "The Validity of the Transport Approximation in Fast-Reactor Calculations," *ANS Transactions,* Vol. 6, No. 1, June, 1963.
13. Flatt, H. P., Baller, D. C., and Cohen, E. R., *AIM*-5. "A multigroup, One-Dimensional Diffusion Equation Code," *NAA-SR*-4694, March 1, 1960.
14. Garelis, E., "Treatment of Annular Voids in Diffusion Theory," *Nuclear Science and Engineering,* Vol. 12, April, 1962.
15. Velarde, G., "Effective Diffusion Coefficient in Void Regions," *Nuclear Science and Engineering,* Vol. 13, June, 1962.

## ACKNOWLEDGEMENT

The author is indebted to Mr. Jerry P. Davis of the Jet Propulsion Laboratory Advanced Propulsion Engineering Section for many illuminating discussions on the work reported herein, and to Mr. Wilson Silsby, Jr., of the Applied Mathematics Section, for carrying out the digital computer calculations.